Earth Surface Processes and Landforms
Earth Surf. Process. Landforms **23**, 581–594 (1998)

GEOMORPHOLOGICAL SIGNATURES: CLASSIFICATION OF AGGREGATED SLOPE UNIT OBJECTS FROM DIGITAL ELEVATION AND REMOTE SENSING DATA

PHILIP T. GILES*
Department of Geography, Saint Mary's University, Halifax, Nova Scotia, Canada B3H 3C3

Received 10 September 1996; Revised 16 June 1997; Accepted 27 August 1997

ABSTRACT

The concept of a geomorphological signature is developed for classifying and mapping slope units with an automated procedure for analysing digital elevation and remote sensing data. Slope units are extracted from a digital elevation model (DEM) using a break of slope rule on downslope profiles. Each slope unit is an aggregated object of contiguous pixels and is summarized with five suites of variables: shape, topography, topographic variability, spectral characteristics, and variability in spectral characteristics. The variables are derived from the DEM and a corresponding SPOT satellite image.

A ten-class scheme is used to classify slope units for a study area in southwest Yukon, Canada. Discriminant analysis results show the power of various combinations of variables to distinguish the classes, with a maximum classification accuracy of 90 per cent. Training signatures are employed for classifying the entire study area to produce a map with 88·5 per cent accuracy. The study shows that generating extensive geomorphological signatures for aggregated slope unit objects is a valuable exercise for discrimination and mapping. © 1998 John Wiley & Sons, Ltd.

KEY WORDS: geomorphology; slope profiles; remote sensing; digital elevation models; classification; mapping

INTRODUCTION

One of the potential, but as yet underdeveloped, uses of digital remote sensing data is for geomorphological study and landscape interpretation (Pickup, 1990; Young and White, 1995). In particular, satellite imagery should contribute to efforts in geomorphological mapping of large and remote areas by complementing field study and aerial photograph interpretation as described by Kienholz and Bichsel (1982). A problem, however, is that specific geomorphological features are poorly represented as objects by remote sensing pixels having dimensions that are constant and landscape-independent. Features that are larger than the database pixel size require a higher level of reasoning for accurate identification in a remote sensing data matrix. Higher level reasoning in the search for specific geomorphological features may include perceiving feature boundaries using contextual clues (Mackay *et al*., 1992).

A second problem in the use of remote sensing data in geomorphological mapping is that topography is not represented explicitly in the imagery (although there may be valuable implicit expressions of topography as shown by Craig (1984) and by Astaras and Soulakellis (1992)). The lack of explicit topographic information has been solved with studies integrating a digital elevation model (DEM) with remote sensing data. Townsend (1981) outlines the 'logical channel method' where ancillary topographic channels are added to a classification procedure principally based on remote sensing data analysis. The theory is that some distinguishing characteristics of the classes are defined by topographic variables, or that some of the variation in the remote sensing data is caused by topographic variation. Therefore, more complete and more logical descriptions of the classes are generated by adding ancillary topographic channels. Successful application of this theory has been demonstrated by Fleming (1988), Frank (1988), Niemann (1991), Ahmad *et al*. (1992) and Giles *et al*. (1994), each of whom used variables derived from a DEM to increase classification accuracy.

In the process of creating a map by classifying a digital image (e.g. a remote sensing scene) with statistical methods, one step is to generate a set of *class signatures*. The signatures are derived from a selection of

* Correspondence to: P. T. Giles, Department of Geography, Saint Mary's University, Halifax, Nova Scotia, Canada B3H 3C3.

CCC 0197-9337/98/070581–14 $17.50

representative training sites using a number of discriminating variables that are chosen to describe the classes. As implied previously, higher classification accuracy is achieved if the chosen variables describe the distinguishing characteristics of the classes (Swain, 1978; Marceau *et al*., 1994). Therefore, the operator should carefully consider what variables contribute to class signatures that will logically maximize the classification accuracy; in the studies mentioned above this was done by adding topographic variables to a remote sensing data set.

Pike (1988) developed the idea of *geometric signatures* to describe the morphometric characteristics of landscapes using variables derived from DEM analysis. A geometric signature is described as a 'critical analytic tool . . . that describes topographic form well enough to distinguish among geomorphologically disparate landscapes' (Pike, 1988, p. 491). Two terrain types in California were distinguished consistently using a set of 17 topographic variables describing topographic profiles. In an extension of Pike's work, McDermid and Franklin (1995) used slope profile analysis for classification of landscape features in Kluane National Park, Yukon. A set of variables describing the slope profile on which the landscape feature was situated were compared to sets of spectral variables (those describing reflectance values in a remote sensing image) and texture variables (those describing the spatial arrangement of reflectance values in a remote sensing image). Compared to the sets of spectral and texture variables, profile variables produced the highest overall classification accuracy.

Two examples of automated higher level geomorphological reasoning applied to DEMs are by Chorowicz *et al*. (1989) and Mackay *et al*. (1992). Chorowicz *et al*. (1989) used a pattern recognition technique to find strike ridge landforms and fluvial deposits from elementary profile analysis of a DEM. High values of the second derivative along a profile were considered to be geomorphologically significant points and were used in the identification of specific landform features. Mackay *et al*. (1992) sought to recognize glacial troughs and cirques by applying rules about the known form of such features. Both of these studies are examples of how geometric signatures can be used to extract higher level geomorphological features from DEM analysis.

GEOMORPHOLOGICAL SIGNATURES

In this work, a new type of signature is introduced: *geomorphological signatures*. As a development in the field of integrated digital elevation and remote sensing data, this type of signature is designed to exploit complementary information in a DEM *and* a remote sensing image for geomorphological landscape classification. The geomorphological objects in this study are called *slope units*, an idea adapted from the catena principle (Scheidegger, 1986) and the landscape model of Dalrymple *et al*. (1968). Breaks of slope often define where process and slope form change between adjacent units, changes that may also be linked to certain lithological and vegetation characteristics. A slope unit as used here is a section of a cross-sectional downslope profile with upper and lower boundaries located at successive breaks of slope. It is suggested that slope units have certain distinguishing characteristics that can be summarized from a digital data set and used in a procedure to generate a geomorphological map.

The challenge is to create an automated process to identify slope unit boundaries in the digital database and to extract slope units as objects of aggregated pixels prior to classification. There has been considerable previous work on slope profile analysis and the identification of breaks of slope (e.g. Savigear, 1967; Young, 1975; Parsons, 1988). The approach developed for this work (described in a later section) draws upon these previous studies and extends the analysis from profiles surveyed in the field to profiles identified in a grid DEM.

Using breaks of slope to mark the boundaries of slope unit objects is supported by commonly used techniques in geomorphological mapping (Gardiner and Dackombe, 1983; Parsons, 1988). Breaks of slope are often identified as significant topographic features, indicating the boundaries between adjacent geomorphological units on a map. In the present case, slope unit identification is restricted to cross-sectional profiles with a width of one pixel, but the final classified map (shown later) also reveals patches of pixels with the same classification value that can be interpreted to represent individual geomorphological features.

An application of the new process is demonstrated for a moderate to high relief study area in southwest Yukon, Canada. A list of variables (together constituting a geomorphological signature) is used to describe numerically the properties of each aggregated slope unit object in the study area. From the DEM, information is

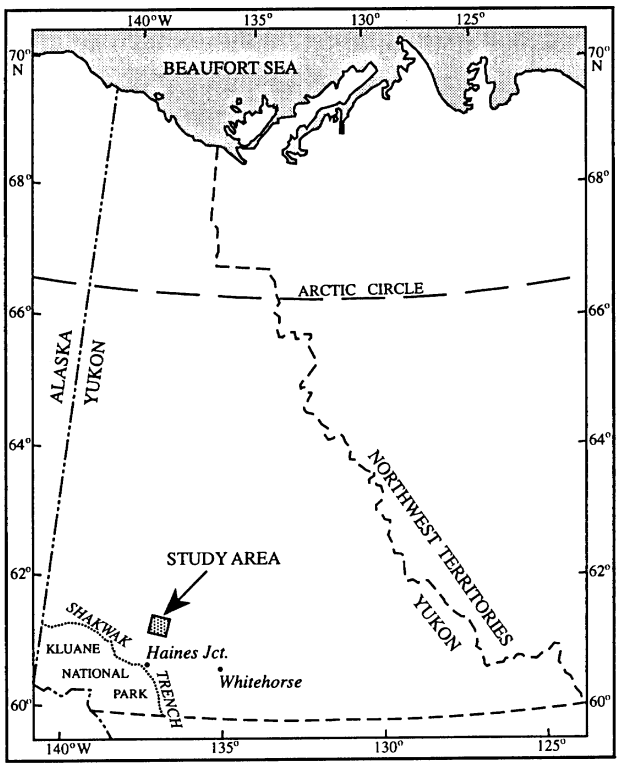

Figure 1. The study area, located in the southwest corner of Yukon Territory, Canada

extracted on the shape and topography of an object, while the SPOT satellite image is the source of information about the visible and near-infrared reflectance characteristics of surface materials. Although lithological materials at the surface are frequently obscured by vegetation in many climatic zones (Adams and Adams, 1984; Warner *et al*., 1994), there is often a strong link between vegetation and the underlying surface (Howard and Mitchell, 1985; Pickup and Chewings, 1996).

The geomorphological signature comprises a list of variables arranged in five suites. First, there are variables describing the *shape* of the aggregated slope unit object, or its overall dimensions independent of landscape position and orientation. *Shape* variables refer to the form of the aggregated object (e.g. length of slope unit from top pixel to bottom pixel). Second, there is a suite of variables describing the *topography* of each of the member pixels. *Topography* is a name for the group of variables that summarize the individual topographic values of all pixels constituting the aggregated object (e.g. mean elevation of the pixels). Third, there are variables summarizing the *spectral* characteristics of the member pixels. Fourth and fifth, there are variables describing the *topographic variability* and *spectral variability* of pixels within the aggregated slope unit object. The contribution of these suites in discriminating the classes is analyzed by submitting various combinations of variables to the statistical classification procedure. After evaluating the discrimination results, one combination of variables is used to generate a classified map of the study area.

DESCRIPTION OF STUDY AREA

The classification and mapping project is conducted for a moderate to high relief study area called the Three Guardsmen Upland in southwest Yukon, Canada (Figure 1). A 20 km×20 km area dominated by slope processes was selected for study. There is an elevation range of 1310 m (820–2130 m) and discontinuous permafrost that increases in occurrence at higher elevations and on more north-facing slopes. Vegetation distribution is related to elevation, slope gradient and aspect (Giles *et al*., 1994), ranging from closed spruce forest on the lowest slopes to bare rock and tundra on flat mountain summits.

Table I. Classification scheme for slope units (values are approximate and typical of the class based on field observations)

	Class label	Description (slope gradient)	Dominant erosion process	Dominant surface material	Dominant vegetation	Other characteristics
1	Headwall	Steep rock face (>40°)	Rockfall erosion	Bedrock	Unvegetated	Occur most frequently in glacier-scoured valleys
2	Cryoplanation Summit	Flat high plateau (<5°)	In-situ infiltration	Boulders; thin discontinuous soil layer	Low tundra plants; lichen	Occur above 1750 m elevation
3	Gelifluction Slope	Upper mountain slope (5–20°)	Lobes of soil creeping downslope by gelifluction	Boulders; soil in lobes	Low tundra plants; lichen; grass	Located above 1650 m elevation
4	Solifluction Slope	Lower mountain slope (5–15°)	Soil creep by frost heave; groundwater sediment transport	Soil	Shrubs; grasses; sparse trees at lower elevations	Become waterlogged in areas of high drainage concentration
5	Debris Cone	Run-out zone and accumulation of loose debris (15–30°)	In-situ frost shattering	Loose angular boulders	Unvegetated	Fresh alluvial and colluvial debris flow accumulation
6	Debris Mantle	Blockfield (5–40°)	In-situ frost shattering and readjustment of slope	Stable and semi-stable boulders	Unvegetated; dark lichens indicate long-term stability	Slopes > angle of repose maintained by interlocking
7	Bluff	Bank of unstable exposed sandy sediment (10–35°)	Slope failure; slope wash; aeolian erosion	Massive silt, sand, gravel and boulder mixture	Unvegetated; grasses	Sediment is from glacio-lacustrine deposition in W. Aishihik Valley
8	Valley Flat	Flat-lying area at lower end of profile (<5°)	In-situ infiltration	Soil and organic deposits	Grasses; shrubs; mosses	Valley flats in W. Aishihik Valley are the river floodplain
9	Hummock Slope	Well-drained isolated slope (<15°)	Stable; slope wash; infiltration	Gravel and boulders	Sparse trees and shrubs; grasses	Deposited as glacial kame moraines in lower flat areas
10	Stable Foot Slope	Lower elevation slope in/bordering W. Aishihik Valley (<10°)	Infiltration; slope wash	Soil	Closed forest	Stable foot slopes in W. Aishihik Valley are on glacio-lacustrine sediment

Hughes (1990) conducted a field-based survey of the surficial geology and geomorphology of the region including the Three Guardsmen Upland. The landscape was influenced by several glacial advances of the Cordilleran Ice Sheet in the Late Wisconsinan period. Ice flowed northward from the St. Elias Mountains filling the lower valleys and leaving nunataks exposed to periglacial processes. In three main valleys glacial action carved steep U-shaped valleys and local sources of ice also created steep cliffs in cirques and tributary valleys. These parts of the landscape are characterized by rapid mass movements and debris cones. As the ice retreated at the end of the last glacial period (9660±150 years BP according to Lowden and Blake (1970)), glacial Lake Sekulmun-Aishihik formed due to drainage to the south being blocked. Today, the West Aishihik River is an underfit stream lying in the glaciated valley on the former glacial lake bottom. Exposed, unstable glaciolacustrine deposits exist on the former glacial lake margins.

Periglacial processes are important geomorphological factors in the Three Guardsmen Upland. Several of the mountain peaks in the area are flat-topped cryoplanation summits, surrounded by zones of gelifluction at the higher elevations and solifluction on lower slopes. A classification scheme consisting of ten classes was created (Table I). Although each class is summarized with a short label, the classes are defined by a general description and characterizations of dominant erosion process, dominant surface material and dominant vegetation.

DESCRIPTION OF DATA

Two complementary Système Probatoire d'Observation de la Terre (SPOT) satellite images were used to generate a DEM using an automated software package. SPOT images were acquired one year apart in multispectral mode. The first image was acquired on 11 August 1989, with a view angle of –27·9° (west-looking). At the time of imaging, the sun azimuth and sun elevation angles were 160·0° and 42·6°, respectively. On 21 July, 1990, the second image was acquired with a complementary view angle of 6·0° (east-looking), sun azimuth of 171·1°, sun elevation of 49·0°. Multispectral SPOT images consist of reflectance data in three bands

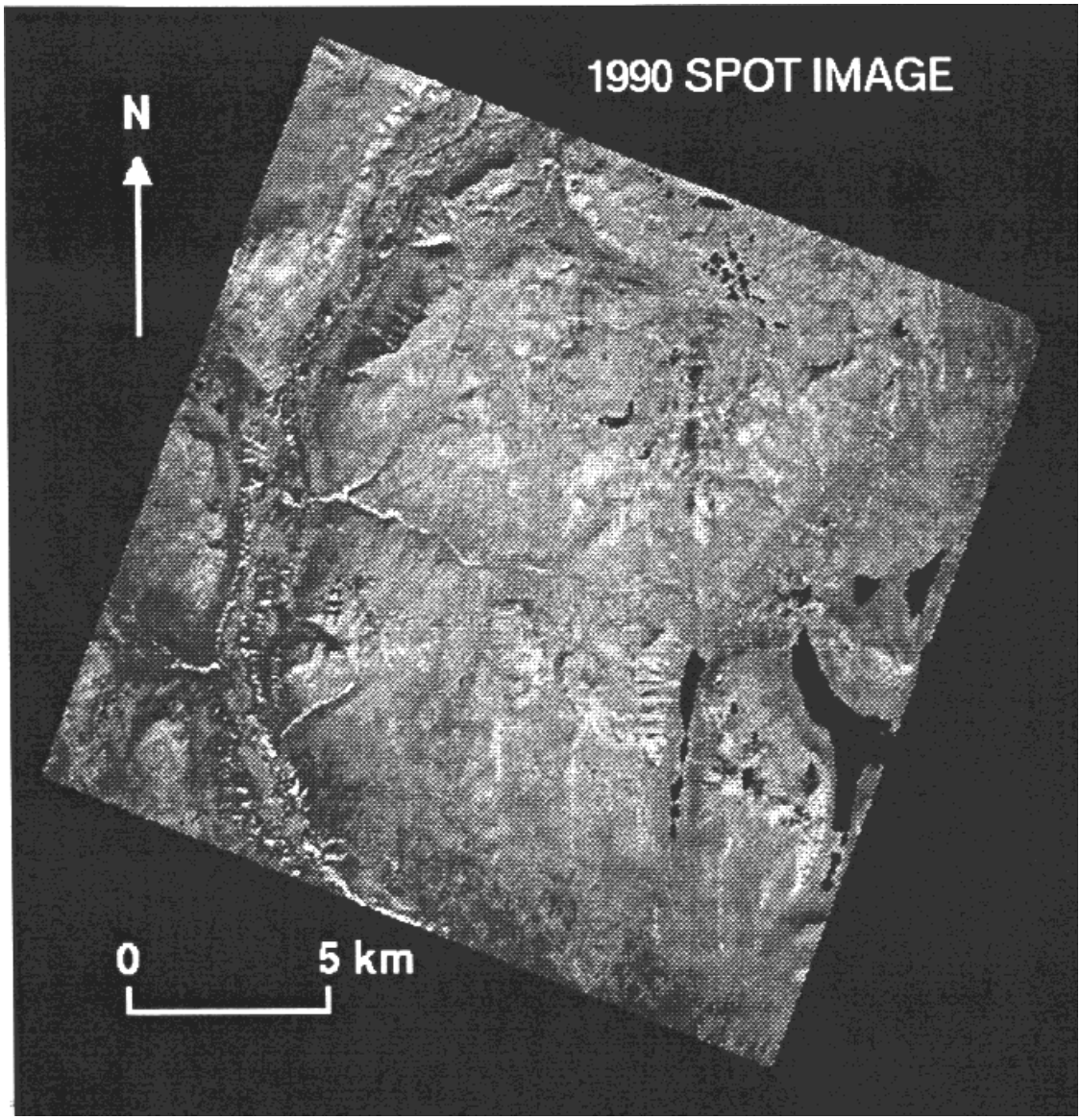

Figure 2. False-colour representation of 1990 SPOT satellite image of the Three Guardsmen Upland study area

of the electromagnetic spectrum: green (0·50–0·59μm), red (0·61–0·68μm) and near-infrared (0·79–0·89μm). The DEM and both images were orthoganalized and georeferenced to the UTM co-ordinate system with a final pixel size of 20 m. Field verification data were collected by the author and an assistant. Later, sites visited in the field were supplemented by sites selected by aerial photograph interpretation for a total of 20 evaluation sites, distributed across the study area, in each of the ten classes.

Although the complementary nature of the two SPOT images was essential to the generation of the DEM, only one SPOT image is used for discrimination and classification. In the automated DEM generation process, a window-matching technique is used to find corresponding pixels in the two images; then the parallax and elevation are estimated in a manner analogous to that developed for aerial photograph photogrammetry. After georeferencing, however, each image contains similar reflectance information in corresponding pixels and subsequent use of both images is unnecessary. There was limited change at the landscape scale over the one-year interval, and only the 1990 SPOT image is used for discrimination and classification purposes. A false-colour representation of the 1990 image is shown in Figure 2.

Table II. Accuracy of DEM and derivative topographic variables. Errors were calculated by subtracting digital estimates from corresponding field measurements. 'Corr.' is the correlation value between two variables, *r*

Variable (units)	Number of sites	Summary of errors				
		Std. dev.	Max.	Min.	Mean	Corr.
Elevation (m)	122	22·6	84·6	–65·3	–3·2	0·998
Slope gradient (degrees)	79	9·6	26·2	–29·8	–1·6	0·66
Incidence value (dimensionless)	79	0·16	0·27	–0·65	0·00	0·78
Profile curvature (m^{-1})	45	0·006	0·015	–0·018	0·000	0·62

Generation of the DEM was described by Giles *et al*. (1994) in an initial test of this type of DEM for use in studies with integrated sets of remote sensing and digital elevation data. The DEM used in this study was evaluated with field measurements of slope gradient, incidence value, and profile curvature to compare with values calculated from the DEM. Because the results showed that there were shortcomings in the accuracy of derivative attributes – particularly profile curvature, a second derivative of elevation – Giles (1996) improved the post-generation DEM processing steps. Table II contains a summary of topographic errors for the final DEM. As discussed by Giles and Franklin (1996), these errors are common for this type of DEM. However, for future projects dedicated to geomorphological mapping, the potential of the automated method described here would be maximized with the most accurate DEM available.

For slope profile studies, 20 m is suggested as the maximum step length that should be used (Gardiner and Dackombe, 1983). In this DEM, grid-normal steps are 20 m in length, while diagonal steps are longer at 28 m. In a DEM with a smaller pixel size, finer landscape features may be represented, but a 20 m DEM was considered to be suitable for a landscape-scale mapping project.

METHOD OF IDENTIFYING SLOPE UNIT OBJECTS

Slope unit objects are embedded in the digital elevation and remote sensing data matrix and must be identified by searching either for boundaries that separate adjacent objects, or for groups of contiguous pixels with some sort of internal homogeneity. In this work, the former approach is followed: slope unit object boundaries are given by breaks of slope on downslope profiles extracted from the DEM. The DEM and remote sensing data are geometrically co-registered with the same pixel size, and boundaries found in the DEM are also supplied to the SPOT image.

Early investigations in slope profile analysis used field surveyed profiles as a data source. In the well known system of best units analysis, Young (1971, 1975) searched for profile units that had similar internal homogeneity of slope gradient (best segments) or of curvature (best elements). Boundaries between units were placed where the internal unit variance exceeded a selected threshold. Savigear (1967) showed that slope profiles could be broken into units separated by discontinuities in adjacent slope angles, while Francou and Mante (1990) showed that profiles could be segmented on the basis of identifying high values of the second derivative of elevation. The method developed here uses a similar characteristic – the change in slope gradient along a cross-sectional profile – to determine where breaks of slope are located. Because a downslope profile extracted from a DEM may contain both grid-normal and diagonal steps, a direct calculation of the second derivative of elevation was abandoned in favour of a calculation of the change in slope gradient along the profile.

In each of the aforementioned slope profile studies, unit boundary identification depended upon a user-selected threshold being exceeded; if the threshold was not exceeded a slope unit boundary was not marked. As shown in the review by Parsons (1988), user-selected thresholds are common in slope profile and slope classification studies. The problem of relying upon a user-selected threshold has not been solved in the present work – an arbitrary threshold value of the change in slope gradient required for the acceptance of a break of slope is still used. In this case, the threshold value (±0·1 radians) was selected on the basis of field measurements in the study area. The method of identifying slope units also addresses some of the problems of calculating a break of slope value in a grid DEM; it is described in detail by Giles and Franklin (1998) and is summarized here briefly. A program to implement the method was written in the C language and executed on a RISC/6000 platform in a UNIX environment.

Table III. List of variables describing aggregated slope unit objects (variables marked with * were calculated but subsequently excluded from discrimination analysis due to high correlations with other variables)

Suite	Variable name	Description
Shape	ELEV-RANGE	Maximum elevation minus minimum elevation
	DIST-FLAT	Planimetric distance following profile
	DIST-PLAN*	Direct planimetric distance from upper to lower end
	DIST-PROF*	Distance following profile accounting for elevation change
	DIST-HYP*	Direct distance from upper to lower end accountin for elev. change
	SHAPE	DIST-PROF divided by DIST-FLAT
	CURV-MEAN	Mean of δ values
Topography	ELEV-MEAN	Mean of elevation values
	SLOPE-MEAN	Mean of slope gradient values
	INC-MEAN	Mean of incidence values
Topographic variability	SLOPE-SD	Standard deviation of slope gradient values
	INC-SD	Standard deviation of incidence values
Spectral characteristics	SPOT1-MEAN	Mean of SPOT band 1 digital numbers
	SPOT2-MEAN*	Mean of SPOT band 2 digital numbers
	SPOT3-MEAN	Mean of SPOT band 3 digital numbers
	NDVI-MEAN	Mean of NDVI values
Spectral variability	SPOT1-SD	Standard deviation of SPOT band 1 digital numbers
	SPOT2-SD*	Standard deviation of SPOT band 2 digital numbers
	SPOT3-SD	Standard deviation of SPOT band 3 digital numbers
	NDVI-SD	Standard deviation of NDVI values

Processing prior to slope unit identification involves labelling pixels with drainage accumulation of at least $8{\cdot}0\times10^5$ m^2 (2000 pixels) as stream pixels. The stream threshold value was selected based on observations of stream channel heads in the study area. A list of seed pixels is then supplied by the user, for which corresponding slope units are identified. Seed pixels used here are the evaluation sites distributed across the study area identified from field verification and aerial photograph interpretation. The first step for each seed pixel is to find a full-length slope profile using steepest ascent and descent rules. Profiles are followed upslope from the seed pixel to a pixel with zero drainage accumulation input (a local topographic high), and downslope to a stream pixel where there is a change from slope processes to fluvial processes. Breaks of slope are identified by calculating the change in slope gradient along the profile. Those pixels for which the change in slope gradient exceeds the threshold are marked as breaks of slope. The selection of the break of slope threshold value, $\pm0{\cdot}1$ radians, was guided by field measurements of profile curvature made by the author on profiles with 20 m steps. As part of the DEM evaluation exercise (see Table II), field measurements of profile curvature were made at selected locations judged to be breaks of slope based on the author's previous experience in topographic profiling.

A slope unit is extracted as the linear group of pixels lying on the profile between the next higher and next lower breaks of slope from the current seed pixel. The slope unit can be summarized by the shape of the overall object and by the characteristics of the member pixels. Table III contains the list of variables describing aggregated slope units, divided into five suites: shape, topography, topographic variability, spectral characteristics, and variability in spectral characteristics. Thus, for each slope unit extracted from the digital database, a geomorphological signature of 20 variables is generated. The Normalized Difference Vegetation Index (NDVI) is a measure of the amount of biomass at a given pixel location calculated as the normalized difference between near-infrared reflectance (SPOT band 3) and red reflectance (SPOT band 2) (Ustin *et al.*, 1994). Analysis showed that some pairs or groups of the 20 variables had correlation values greater than 0·95. To reduce data redundancy only one variable from a pair or group of highly correlated variables was entered into the discrimination procedure. This action reduced the geomorphological signature used in discrimination from 20 variables to 15 variables. Of the 15 remaining variables, no pairwise correlation value exceeded 0·80.

In a study with similar goals to this work (landscape segmentation into geomorphometric units), Dymond *et al.* (1995) used a break of slope rule to identify 'land components'. In the downslope direction, land component boundaries were identified by iteratively dividing an aspect region class (classes with arbitrary boundaries at

Table IV. Combinations of variables describing aggregated slope units used in discriminant analysis

Combination	Suites	Variables included
1	Spectral characteristics	SPOT1-MEAN, SPOT3-MEAN, NDVI-MEAN
2	Spectral characteristics Spectral variability	SPOT1-MEAN, SPOT3-MEAN, NDVI-MEAN, SPOT1-SD, SPOT3-SD, NDV1-SD
3	Topography	ELEV-MEAN, SLOPE-MEAN, INC-MEAN
4	Topography Topographic variability	ELEV-MEAN, SLOPE-MEAN, INC-MEAN, SLOPE-SD, INC-SD
5	Topography Spectral characteristics	ELEV-MEAN, SLOPE-MEAN, INC-MEAN, SPOT1-MEAN, SPOT3-MEAN, NDVI-MEAN
6	Shape	ELEV-RANGE, DIST-FLAT, SHAPE, CURV-MN
7	Shape Topography	ELEV-RANGE, DIST-FLAT, SHAPE, CURV-MN, ELEV-MEAN, SLOPE-MEAN, INC-MEAN
8	Shape Topography Spectral characteristics	ELEV-RANGE, DIST-FLAT, SHAPE, CURV-MN, ELEV-MEAN, SLOPE-MEAN, INC-MEAN, SPOT1-MEAN, SPOT3-MEAN, NDV1-MEAN
9	Shape Topography Spectral characteristics Topographic variability Spectral variability	ELEV-RANGE, DIST-FLAT, SHAPE, CURV-MN, ELEV-MEAN, SLOPE-MEAN, INC-MEAN, SPOT1-MEAN, SPOT3-MEAN, NDVI-MEAN, SLOPE-SD, INC-SD, SPOT1-SD, SPOT3-SD, NDV1-SD

Table V. Summary of classification accuracy from discriminant analysis using variables describing aggregated slope units: full evaluation set (20 sites per class)

Variable combination	Class producer's accuracy (%)										Overall (%) (95% conf. limits)		Kappa
	1	2	3	4	5	6	7	8	9	10			
1	65	65	60	75	25	20	80	35	60	95	58·0	(51·4, 64·6)	0·53
2	60	70	55	85	30	35	85	35	70	100	62·5	(56·0, 69·0)	0·58
3	95	100	70	50	45	75	80	60	40	50	66·5	(60·1, 72·9)	0·63
4	90	100	60	50	40	90	65	60	60	45	66·0	(59·6, 72·4)	0·62
5	95	100	80	95	55	80	100	65	70	90	83·0	(77·9, 88·1)	0·81
6	75	25	50	25	55	45	45	60	75	25	48·0	(41·3, 54·7)	0·42
7	90	100	85	60	70	65	70	70	90	70	77·0	(71·3, 82·7)	0·74
8	90	100	85	95	70	70	100	65	85	95	85·5	(80·8, 90·2)	0·84
9	90	100	85	100	90	70	95	75	95	100	90·0	(86·0, 94·0)	0·89

45° intervals) into upper and lower slope components. Boundaries were determined implicitly by assuming that a land component had approximately constant slope gradient values; when the variance in slope gradient exceeded a user-selected threshold, a boundary was marked. The result was a map consisting of polygons (consisting of at least 100 pixels) with similar internal topographic characteristics. In the present study, slope units are restricted to one pixel in width along profile cross-sections but comparable map output to that of Dymond *et al*. (1995) is achieved, as explained in a later section on map production.

RESULTS OF DISCRIMINATION ANALYSIS

Using the discriminant analysis package in SPSS statistical software (Norusis and SPSS, 1990), ten combinations of the five suites of variables are submitted for site classification as shown in Table IV. Initial evaluation of the power of the various combinations to discriminate the ten slope unit classes is done with all 200 sites; in this case the same set of 20 sites per class is used for both training *and* testing. This approach uses the maximum information available to train the geomorphological class signatures, but the accuracy of the subsequent classification (Table V) will probably be overestimated (Congalton, 1991). Therefore, two tests are

Table VI. Summary of classification accuracy from discriminant analysis using variables describing aggregated slope units

Variable combination	Class producer's accuracy (%)										Overall (%) (95% conf. limits)		Kappa
	1	2	3	4	5	6	7	8	9	10			
(a) Testing set A (five sites per class)													
1	80	40	80	80	20	0	80	80	20	100	52·0	(36·8, 67·2)	0·47
2	60	60	60	100	0	20	80	40	60	100	58·0	(43·0, 73·0)	0·53
3	100	100	100	60	60	100	100	80	40	80	82·0	(70·3, 93·7)	0·80
4	100	100	80	60	20	100	60	60	60	60	70·0	(56·0, 84·0)	0·67
5	80	100	100	80	60	80	100	60	40	80	78·0	(65·4, 90·6)	0·76
6	40	20	100	20	80	80	40	100	60	20	54·0	(38·8, 69·2)	0·49
7	100	100	100	40	80	80	80	100	80	80	84·0	(72·8, 95·2)	0·82
8	80	100	100	80	60	80	100	100	100	100	90·0	(80·9, 99·1)	0·89
9	80	100	100	80	80	80	100	100	100	100	92·0	(83·7, 100·0)	0·91
(b) Testing set B (five sites per class)													
1	40	80	40	60	40	40	100	40	20	80	54·0	(38·8, 69·2)	0·49
2	40	60	40	60	20	40	80	60	80	80	56·0	(40·9, 71·1)	0·51
3	80	100	40	20	60	20	40	60	60	40	52·0	(36·8, 67·2)	0·47
4	80	100	40	40	80	40	60	40	60	40	58·0	(43·0, 73·0)	0·53
5	80	100	40	80	80	40	100	40	60	80	70·0	(56·0, 84·0)	0·67
6	100	20	20	40	60	20	20	80	100	0	46·0	(30·8, 61·2)	0·40
7	80	100	60	40	100	60	40	40	100	60	68·0	(53·8, 82·2)	0·64
8	80	100	60	80	80	60	100	80	80	80	80·0	(67·8, 92·2)	0·78
9	80	100	60	80	60	60	80	80	100	80	78·0	(65·4, 90·6)	0·76

performed by splitting the 20 sites per class into two sets: an independent set of five randomly selected sites per class (Tables VIa and VIb), using the remaining 15 sites per class as the signature training set. For overall accuracy, an interval at a 95 per cent level of confidence is calculated, as is the kappa coefficient (a measure of classification accuracy in comparison to the performance of a random classifier (Lillesand and Kiefer, 1994).

Table V shows that as the list of discriminating variables is expanded, the overall classification accuracy generally increases. With three mean spectral variables, the overall accuracy is 58·0 per cent. When the within-unit spectral variability suite is included, an increase of 4·5 per cent is achieved (although the 95 per cent confidence intervals overlap considerably). An increase in overall accuracy is not found by adding the topographic variability suite to the mean topographic variables, as the accuracy is reduced from 66·5 to 66·0 per cent. (When class accuracies decrease in such a case, the additional variables actually create confusion between classes instead of producing a more clear discrimination.) The complementary nature of spectral and topographic information is indicated by the overall accuracy of 83·0 per cent when both suites are entered into the discriminant procedure.

Combination 6 is the suite emphasizing shape variables and 48·0 per cent of the sites are classified correctly. Classification based upon the shape and topographic suites (Combination 7), which are variables all derived from the DEM, improves the accuracy to 77·0 per cent. The two most accurate combinations of variables shown in Table V are those that combine information about the spectral, shape and topographic nature of slope units. Combination 8 omits the suites describing within-unit variability, and the overall accuracy is 85·5 per cent. The final combination includes all five suites – the most extensive geomorphological signatures – to achieve an accuracy of 90·0 per cent.

Tables of results for the test sets of five sites per class (Tables VIa and VIb) are provided for verification of the results in Table V. Supporting evidence about the pattern of increases in accuracy in response to additional variables is provided by the test sets. With fewer sites classified, the confidence intervals are wider than for the full data set. Confidence intervals for the two test sets overlap each other and the interval for the full set with every combination except for Combination 3. In that case, Test Set A has an overall accuracy of 82·0 per cent, so those 50 sites are well discriminated by topographic variables alone. However, Test Set B has an accuracy of 52·0 per cent and the confidence interval does not overlap with Test Set A, although both test set intervals do overlap with the full set.

Examination of individual classes in Table V shows how some classes are classified more accurately with certain suites of variables. For example, Class 5 (Debris Cone) has only 25 per cent correctly classified with the mean spectral variables, but 45 per cent of the sites are correct with the mean topographic variables alone. This class reaches a highest value of 90 per cent correct using the full geomorphological signatures. Other classes, such as Class 10 (Stable Foot Slope), are discriminated accurately by spectral variables alone (95–100 per cent) but not as well by geomorphometric suites (e.g. 50 per cent for topographic variables and only 25 per cent for the shape variables). The idea of employing full geomorphological signatures is to maximize the classification accuracy of all sites by using the most complete description of slope units. Alternatively, these results suggest that various classes are better discriminated by variables extracted from different sources – the DEM, SPOT satellite data, or both.

CLASSIFICATION MAP

The slope unit identification and discrimination procedures can be extended to produce a classified map of the study area. A modified version of the computer program summarized previously is used to extract and summarize the slope units for map production; the difference is that instead of a short list of distributed seed pixels used for discrimination testing (200 sites), each pixel in the study area is now selected in turn to be the seed pixel. Each pixel must be selected as the seed because each pixel potentially lies on a unique slope profile. For the full study area, 20 km×20 km, one million pixels are used as seed pixels. Boundary effects for seed pixels near the edge of the study area are eliminated by including a buffer zone (containing the full complement of digital data) into which the slope profile can extend if necessary in order to reach a stream pixel. Pixels in the buffer zone itself are not used as seed pixels for classification.

Tom and Miller (1984) provide evidence that discriminant analysis can be used to classify digital landscape data instead of the more common maximum likelihood approach to classification. Discriminant functions for classifying the full study area are derived from the 200 sites used to obtain the results in the previous section. The class to which each slope unit (and all of its member pixels) is assigned is stored in an output file, and the information is converted to an image file with a custom program for post-classification.

Because the output image display consists of pixels, a single class value must be determined for each pixel prior to display. A common characteristic of natural landscapes – flow convergence and divergence – presents a new problem for the preparation of the classified map. During classification of the full study area, an individual pixel is likely to be identified as a member of several overlapping slope unit objects from different seed pixels, and these slope units could be assigned to different classes by the discriminant procedure. Therefore, a summary is kept for each pixel, where the class is recorded for each slope unit of which the pixel is a member (i.e. a class frequency histogram is constructed for each pixel). The class displayed on the map for each pixel is then determined by the greatest frequency on the histogram. Although the final map is displayed on a per-pixel basis, the classification was performed on an aggregated slope unit object for each seed pixel.

The problem of pixels existing on more than one slope unit with different classes is created by the act of classification. By having ten classes, each slope unit is forced to fit a user-defined classification where the classes have certain dominant characteristics (Table I). In the landscape, however, each part of the landscape may be affected by multiple processes and may attain a composite form and appearance. This problem of mixed objects is well known in remote sensing, and more advanced techniques of classification (such as mixture modelling and fuzzy classification) are currently under development. The solution used here is to display each pixel as the class with which it is most frequently associated.

In the previous section, the individual class accuracy resulting from discriminant analysis and classification was the *producer's accuracy*, or the percentage of objects of known class membership that were classified correctly. For map evaluation a second type of accuracy will also be presented: the *user's accuracy*, or the percentage of objects assigned to a given class that are in fact known to belong to that class. User's accuracy is a measure of map reliability and is 'indicative of the probability that a pixel classified on the map/image actually represents that category on the ground' (Congalton, 1991, p. 37).

A standard step executed on a raw classified image is to apply a mode filter to reduce the 'salt-and-pepper' appearance or noisy appearance of the image (Lillesand and Kiefer, 1994; Russ, 1995). There is a suggestion

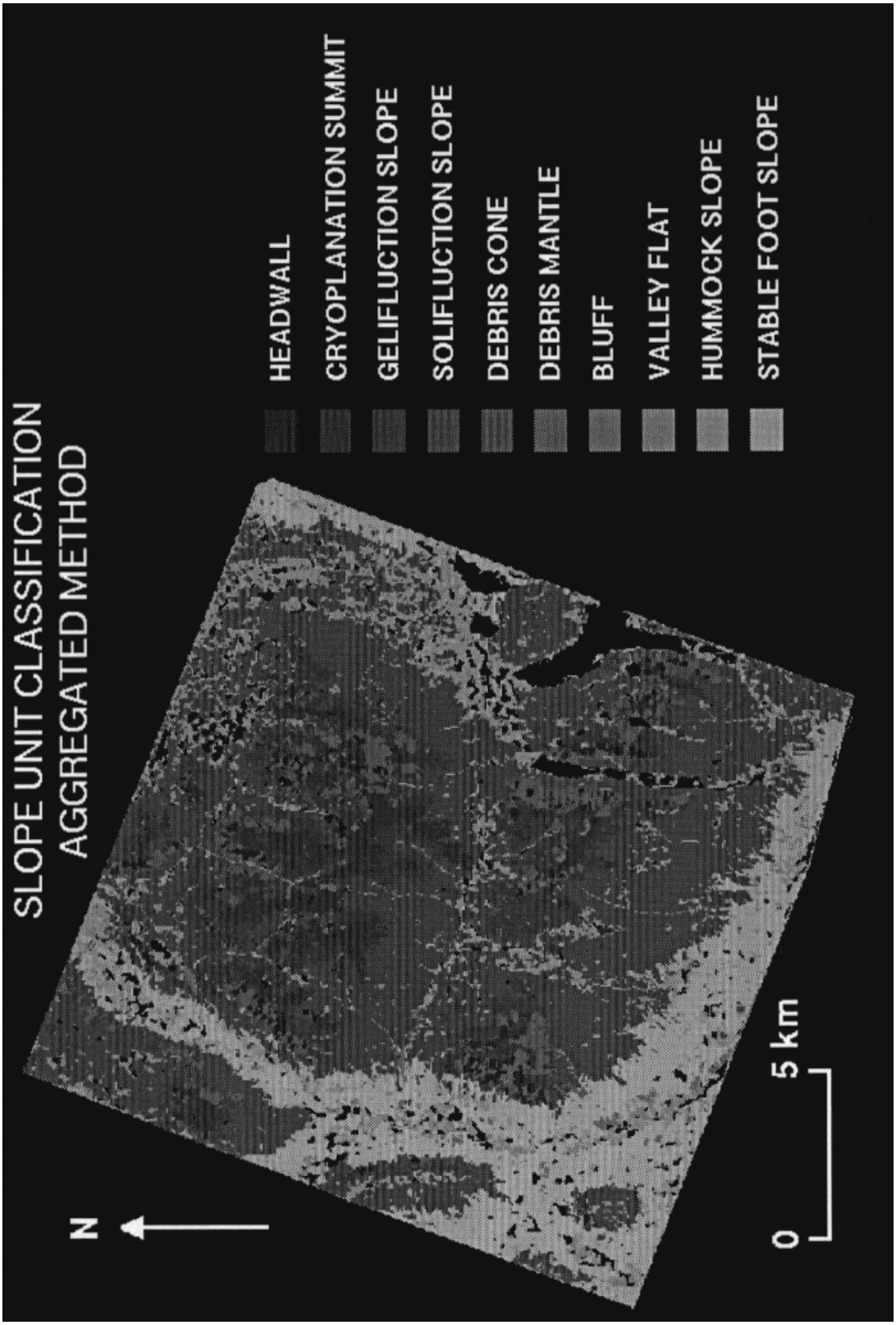

Figure 3. Slope unit classification map of the study area

Table VII. Summary of classification map accuracy using variables describing aggregated slope units (20 sites per class)

Method of calculation	Class accuracy (%)										Overall (%) (95% conf. limits)	Kappa
	1	2	3	4	5	6	7	8	9	10		
(a) Unfiltered image												
Producer's accuracy	90	100	85	100	85	85	95	70	95	100	90·5 (86·6, 94·4)	0·89
User's accuracy	90	100	90	95	90	81	100	93	76	95		
(b) 3×3 mode filtered image												
Producer's accuracy	85	100	85	100	80	75	90	75	95	100	88·5 (84·2, 92·8)	0·87
User's accuracy	89	100	89	87	80	71	100	100	79	95		

Table VIII. Summary of class areas on classified slope unit image (after 3×3 mode filter)

Class	Area ($m^2 \times 10^3$)	Percentage
1	6940	1·6
2	20100	4·7
3	45760	10·7
4	173180	40·3
5	9340	2·2
6	14720	3·4
7	3120	0·7
8	15300	3·6
8	40780	9·5
10	73460	17·1
Stream	6200	1·4
Lake	8020	1·9
Unclass.	12980	3·0
Total	429900	100

that applying a mode filter to a noisy image might also correct some classification errors (Booth *et al*., 1989) because the spatial context of surrounding pixels is taken into account. A 3×3 mode filter was applied to the raw classified image to produce the image displayed in Figure 3.

Classification results for the 200 evaluation sites in the raw classified and mode filtered images are contained in Table VII. The filtered image has been reduced in noisiness, but the overall classification accuracy decreased from 90·5 to 88·5 per cent as a result. The map producer of Figure 3 is at least 85 per cent confident that known pixels are correctly classified in nine out of ten classes, based on Table VIIb. The remaining class, Class 8 (Valley Flat), has a producer's accuracy of only 70 per cent. A user of the classification map would be at least 90 per cent confident in the accuracy of a given pixel for eight of the ten classes. The lower accuracies are in Class 6 (Debris Mantle) with 81 per cent and Class 9 (Hummock Slope) with 76 per cent.

To complete the statistical examination of the classification map, an analysis of class areas was conducted on the image in Figure 3 and is summarized in Table VIII. The largest class by area is Class 4 (Solifluction Slope) with nearly 40 per cent coverage, and the smallest area is covered by Class 7 (Bluff) with less than 1 per cent. There are some unclassified pixels because the method failed in flat areas of the landscape (i.e. seed pixels calculated as having zero slope where a downslope profile could not be followed).

There are points of interest in the spatial characteristics of the classification map (Figure 3). First, the dominance of Class 4 (Solifluction Slope) is evident; recall that this class accounted for about 40 per cent of the pixels. Second, cryoplanation summits (Class 2) tend to be bordered by gelifluction slopes (Class 3), and gelifluction slopes tend to be portrayed adjacent to (and upslope from) solifluction slopes (Class 4). This is a correct representation of the spatial distribution of forms and processes in the Three Guardsmen Upland. Third, some individual geomorphological features can be identified as contiguous pixels with the same class, particularly debris cones (Class 5) and bluffs (Class 7). Fourth, to an observer who has knowledge of the study area, the classification method appears to have more trouble accurately discriminating headwalls (Class 1) and debris mantles (Class 6) than is suggested in the classification tables. Finally, class agglomeration in patches

creates a map in which individual geomorphological features can be identified such as debris cones and headwall cliffs. The map approaches the output of Dymond *et al*. (1995), although in that case each land component (GIS polygon) is entirely class-homogeneous inside its boundary.

SUMMARY

A classification map of slope units was generated for the Three Guardsmen Upland in southwest Yukon, Canada, using automated analysis of digital elevation and remote sensing data. To maximize classification accuracy, geomorphological signatures of ten slope unit classes were generated from training sites. A custom method was used to identify slope units in a DEM prior to classification. On downslope profiles, slope units were found by locating breaks of slope where the change in slope gradient along the profile exceeded a threshold value. Slope units were then extracted as an aggregated group of contiguous pixels between successive breaks of slope. Several of the discriminating variables for describing slope units were derived from DEM analysis, while others came from a co-registered SPOT multispectral satellite image.

Results from discriminant analysis showed that the most accurate overall description of test sites (90 per cent correct) was given by geomorphological signatures consisting of five suites of variables summarizing slope units: shape, topography, topographic variability, spectral characteristics, and variability in spectral characteristics. Other combinations of these suites demonstrated the power of certain types of variables to discriminate with different levels of accuracy, and that overall accuracy generally increased with the inclusion of more information. The results support the continued development of automated methods using integrated digital data sets and higher levels of geomorphological reasoning for mapping large areas.

COLOUR FIGURES

Figure 2 and Figure 3 may be viewed in colour at: http://www.stmarys.ca/academic/arts/geography/faculty/pg.htm

ACKNOWLEDGEMENTS

The author was supported by a Natural Sciences and Engineering Research Council of Canada Postgraduate Scholarship and a Killam Memorial Scholarship from the University of Calgary. Financial support from the Department of Indian and Northern Affairs Northern Scientific Training Program and from the Canadian Circumpolar Institute for logistical expenses is gratefully acknowledged. Valuable guidance was given by Dr Steven Franklin, and field assistance was provided by Daren Trudeau and Mike Wulder. The comments of two anonymous reviewers are also appreciated.

REFERENCES

Adams, J. B. and Adams, J. D. 1984. 'Geologic mapping using LANDSAT MSS and TM images: Removing vegetation by modelling spectral mixtures', *Proceedings, International Symposium on Remote Sensing of Environment, Third Thematic Conference, Remote Sensing for Exploration Geology*, 615–622.

Ahmad, W., Jupp, L. B. and Nunez, M. 1992. 'Land cover mapping in a rugged terrain area using Landsat MSS data', *International Journal of Remote Sensing*, **13**, 673–683.

Astaras, T. A. and Soulakellis, N. A. 1992. 'Contribution of digital image analysis techniques on Landsat-5 TM imageries for drainage network delineation. A case study from the Olympus Mountain, W. Macedonia, Greece', in *Remote Sensing from Research to Operation: Proceedings of the 18th Annual Conference of the Remote Sensing Society*, Dundee, UK, 163–172.

Booth, D. J., Chidley, T. R. E. and Collins, W. G. 1989. 'Integration of context classifiers with GIS', *Proceedings of IGARSS '89/12th Canadian Symposium on Remote Sensing*, Vancouver, Vol. 2, 656–659.

Chorowicz, J., Kim, J., Manoussis, S., Rudant, J.-P., Foin, P. and Veillet, I. 1989. 'A new technique for recognition of geological and geomorphological patterns in digital terrain models', *Remote Sensing of Environment*, **29**, 229–239.

Congalton, R. G. 1991. 'A review of assessing the accuracy of classifications of remotely sensed data', *Remote Sensing of Environment*, **37**, 35–46.

Craig, R. G. 1984. 'The spatial structure of terrain: A process signal in satellite digital images', *Proceedings, IEEE Pecora 9 Symposium, Silver Springs, Maryland*, 51–54.

Dalrymple, J. B., Blong, R. J. and Conacher, A. J. 1968. 'A hypothetical nine-unit landsurface model', *Zeitschrift fur Geomorphologie*, **12**, 60–76.

Dymond, J. R., DeRose, R. C. and Harmsworth, G. R. 1995. 'Automated mapping of land components from digital elevation data', *Earth Surface Processes and Landforms*, **20**, 131–137.
Fleming, M. D. 1988. 'An integrated approach for automated cover-type mapping of large inaccessible areas in Alaska', *Photogrammetric Engineering and Remote Sensing*, **54**, 357–362.
Francou B. and Mante, C. 1990. 'Analysis of the segmentation in the profile of alpine talus slopes', *Permafrost and Periglacial Processes*, **1**, 53–60.
Frank, T. D. 1988. 'Mapping dominant vegetation communities in the Colorado Rocky Mountain Front Range with Landsat Thermatic Mapper and digital terrain data', *Photogrammetric Engineering and Remote Sensing*, **54**, 1727–1734.
Gardiner, V. and Dackombe, R. 1983. *Geomorphological Field Manual*, Allen & Unwin, London 254 pp.
Giles, P. T. and Franklin, S. E. 1996. 'Comparison of derivative surfaces of a DEM generated from stereoscopic SPOT images with field measurements', *Photogrammetric Engineering and Remote Sensing*, **62**(10), 1165–1171.
Giles, P. T. and Franklin, S. E. 1998. 'An automated approach to geomorphological classification using digital data', *Geomorphology*, **21**, 251–264.
Giles, P. T., Chapman, M. A. and Franklin, S. E. 1994. 'Incorporation of DEMs derived by stereocorrelation of satellite imagery in automated terrain analysis', *Computers and Geosciences*, **20**, 441–460.
Howard, J. A. and Mitchell, C. W. 1985. *Phytogeomorphology*, John Wiley & Sons, New York, 222 pp.
Hughes, O. L. 1990. *Surficial Geology and Geomorphology, Aishihik Lake, Yukon Territory*, Geological Survey of Canada Paper **87–29**, 23 pp.
Kienholz, H. and Bichsel, M. 1982. 'The use of air photographs for mapping natural hazards in mountainous areas: A study based on the Colorado Rocky Mountains, U.S.A.', *Mountain Research and Development*, **2**, 349–358.
Lillesand, T. M. and Kiefer, R. W. 1994. *Remote Sensing and Image Interpretation*, 3rd edn, John Wiley & Sons, New York, 750 pp.
Lowden, J. A. and Blake, W. 1970. *Geological Survey of Canada Radiocarbon Dates IX*. Geological Survey of Canada, Paper **70–2**, Part B, 86 pp.
Mackay, D. S., Robinson, V. B. and Band, L. E. 1992. 'Classification of higher order topographic objects on digital terrain data', *Computers, Environment and Urban Systems*, **16**, 473–496.
Marceau, D. J., Howarth, P. J. and Gratton, D. J. 1994. 'Remote sensing and the measurement of geographical entities in a forested environment. 1. The scale and spatial aggregation problem', *Remote Sensing of Environment*, **49**, 93–104.
McDermid, G. J. and Franklin, S. E. 1995. 'Remote sensing and geomorphometric discrimination of slope processes', *Zeitschrift fur Geomorphologie*, Supplementband **101**, 165–185.
Niemann, K. O. 1991. 'Landscape drainage modelling to enhance Landsat classification accuracies', *Geocarto International*, **6**, 13–30.
Norusis, M. J. and SPSS Inc. 1990. *SPSS Advanced Statistics User's Guide*, Chicago, 285 pp.
Parsons, A. J. 1988. *Hillslope Form*, Routledge, London, 212 pp.
Pickup, G. 1990. 'Remote sensing of landscape processes', in Hobbs, R. J. and Mooney, H. A. (Eds), *Functioning*, Springer-Verlag, New York, Ch. 11, 221–247.
Pickup, G. and Chewings, V. H. 1996. 'Correlations between DEM-derived topographic indices and remotely-sensed vegetation cover in rangelands', *Earth Surface Processes and Landforms*, **21**, 517–529.
Pike, R. J. 1988. 'The geometric signature: Quantifying landslide-terrain types from digital elevation models', *Mathematical Geology*, **20**, 491–511.
Rouse, J. W., Haas, R. H., Schell, J. A. and Deering, D. W. 1973. 'Monitoring vegetation systems in the Great Plains with ERTS'. *Proceedings, Thirds ERTS Symposium*. NASA Special Publication 351, 309–317.
Russ, J. C. 1995. *The Image Processing Handbook*, Lewis Publishers, Boca Raton, Florida, 696 pp.
Scheidegger, A. E. 1986. 'The catena principle in geomorphology', *Zeitschrift fur Geomorphologie*, **30**, 257–273.
Swain, P. H. 1978. 'Fundamentals of pattern recognition in remote sensing', in Swain, P. H. and Davis, S. M. (Eds), *Remote Sensing: The Quantitative Approach*, McGraw-Hill Book Company, New York, Ch. 3, 136–187.
Tom, C. H. and Miller, L. D. 1984. 'An automated land-use mapping comparison of the Bayesian maximum likelihood and linear discriminant analysis algorithms', *Photogrammetric Engineering and Remote Sensing*, **50**, 193–207.
Townshend, J. R. G. 1981. 'Image analysis and interpretation for land resources survey', in Townshend, J. R. G. (Ed.), *Terrain Analysis and Remote Sensing*, George Allen & Unwin, London, Ch. 4, 59–108.
Ustin, S. L., Szeto, L.-H., Xiao, Q.-F., Hart, J. and Kasischke, E. S. 1994. 'Vegetation mapping of forested ecosystems in interior central Alaska', in *Proceedings of the 1994 International Geoscience and Remote Sensing Symposium, Part 1*, IEEE, Piscataway, New Jersey, 229–231.
Warner, T. A., Levandowski, D. W., Bell, R. and Cetin, H. 1994. 'Rule-based geobotanical classification of topographic, aeromagnetic, and remotely sensed vegetation community data', *Remote Sensing of Environment*, **50**, 41–51.
Young, A. 1971. 'Slope profile analysis: the system of best units', in Brunsden, D. (Ed.), *Slopes; Form and Process*, Institute of British Geographers Special Publication No. **3**, 1–13.
Young, A. 1975. *Slopes*, Longman, London, 288 pp.
Young R. W. and White, K. L. 1994. 'Satellite imagery analysis of landforms: Illustrations from southeastern Australia', *Geocarto International*, **2**, 33–44.

